JOURNAL OF MATERIALS SCIENCE 22 (1987) 826–834

Some aspects on the microstructure and crystallization of rapidly solidified Al–27% Mn alloy

F. H. SAMUEL*, A. M. SAMUEL
Laboratoire de Physique du Solide, Ecole des Mines, Parc de Saurupt, 54042 Nancy Cedex, France

In a previous paper we reported observations of the icosahedral quasistructure ($m\bar{3}\bar{5}$ symmetry) in Al–14 wt% Mn ribbons. In this paper, the microstructure of rapidly solidified Al–27 wt% Mn ribbons is studied where, in addition to the icosahedral phase, the decagonal quasistructure (10/m or 10/m m m symmetry) is also found to occur along with the equilibrium Al_6Mn and Al_4Mn phases, as well as Al. The effect of annealing (in the range 400 to 600° C for 1 to 100 h) on the stability of these structures was studied, using X-ray diffraction and transmission electron microscopy. While the icosahedral phase becomes unstable at 400° C and crystallizes into Al_6Mn, the decagonal phase is seen to persist even after 500° C/100 h. The existence of the decagonal phase at 600° C together with the Al_4Mn phase suggests that the decagonal phase arises from a commensurate → incommensurate transformation due to atomic displacement within the Al_4Mn phase.

1. Introduction

The rapid solidification of Al–Mn alloys has been a subject of widespread interest, especially in the last two years, since the occurrence of quasistructures was first reported in these alloys [1]. These metastable, quasiperiodic structures or "quasicrystals" as they are called are characterized by long-range orientational order which is inconsistent with lattice translations, and are similar to each other. While the icosahedral phase, exhibiting icosahedral point group symmetry, has been repeatedly observed and studied, other phases like the T, T′, T″, G, G′ and G″ quasistructure phases have also been reported along with the stable Al_6Mn and Al_4Mn phases [2, 3].

Amongst these phases, there is a striking resemblance of diffraction patterns between the icosahedral and T phases. The T phase is believed to result from the former, especially at higher concentrations of magnesium ($\gtrsim$ 22 at % Mn). Very recently, Bendersky [4] has elaborated upon the nature of this T phase and he describes it as a decagonal phase with a 10/m or possibly 10/m m m point group symmetry.

In the present investigations, we report our observations of the decagonal phase along with the icosahedral, Al_6Mn and Al_4Mn phases in Al–27 wt % Mn ribbons obtained by the rapid solidification technique. The decagonal phase is seen to persist even after annealing treatments up to 500° C for 100 h as is confirmed from our X-ray and transmission electron microscopic (TEM) analyses. However, in contrast to previous findings, the presence of microtwins in the transmission electron micrographs indicates that the decagonal phase may well be two sets of decagonal phases occurring as plates (and not in the form of cylinders) inclined to each other and to the axis of ten-fold symmetry.

2. Experimental technique

The present work was performed on an Al–27 % Mn master alloy produced by melt spinning (MS) under an inert atmosphere, see phase diagram in Fig. 1. The alloy was spun into ribbons by conventional melt spinning using a Cu–2% Cr wheel (27 cm diameter) as the rotating chill substrate. The melt spinning was done in a chamber under helium atmosphere, using a wheel rotating velocity of 2200 r.p.m. The ribbon width was typically 1000 μm with a thickness lying in the range 15 to 20 μm. The ribbons were annealed at 400, 450, 500 and 600° C for 1 and 100 h each. The samples were sealed in silica tubes evacuated to 10^{-4} torr and then filled with helium. Annealing was then carried out for these samples at the temperatures mentioned.

Detailed metallographic examinations were made on the ribbons at different conditions employing standard scanning electron microscopy (SEM) and transmission electron microscopy (TEM). The foils were investigated in a Jeol 200CX electron microscope operating at 200 kV and using various specimen inclinations. X-ray diffraction patterns were taken using Cu$K\alpha$ radiation from powders (crushed ribbons) pasted on glass plates by means of an amorphous glue.

3. Results and discussion

3.1. As-melt-spun structure

Fig. 2 represents the microstructure through the thickness of the ribbon. It is evident from this micrograph

*Present address: Central Metallurgical Research and Development Institute, El-Tabbin, Helwan, PO Box Iron and Steel, Cairo, Egypt.

0022–2461/87 $03.00 + .12

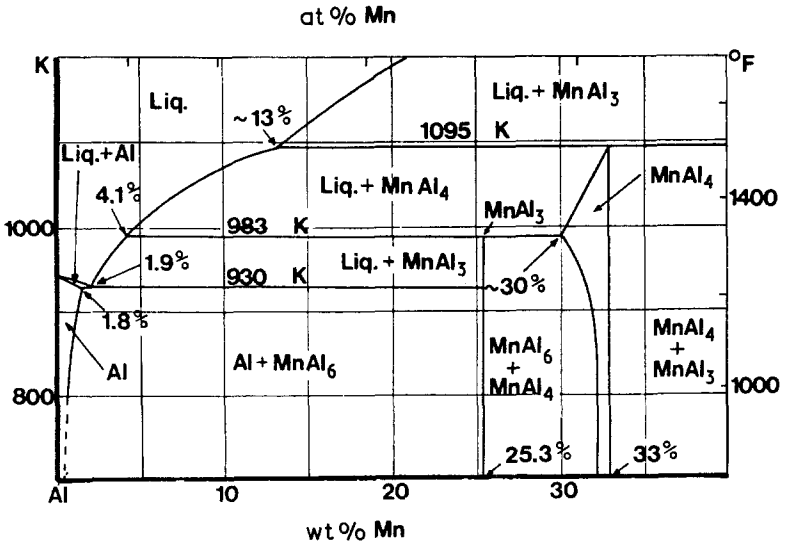

Figure 1 Al–Mn equilibrium diagram.

that there are two distinct zones, zone A (~ 2 to $3\,\mu$m near to the wheel side) and zone B ($\sim 12\,\mu$m). The average Vickers microhardness of zone B was about 5100 to 5200 MPa.

The X-ray powder diffraction pattern revealed the existence of about four phases: Al_4Mn, Al_6Mn, Al and the icosahedral phase, as indexed in Table I. As can be seen from the table, there are three lines which are unindexable on the basis of the currently published data, whereas their relative intensity (i.e. with respect to the peaks of maximum intensity: 0.216 57 and 0.206 in Table I) was seen to be about 5 to 8.

Fig. 3a, taken from zone A, is seen to comprise of many small grains about $0.2\,\mu$m diameter. Moiré fringes were frequently observed at the boundaries between neighbouring grains indicating partial overlapping of these crystals. At a higher level of observation and through zone B, cells belonging to the icosahedral phase (~ 0.1 to $0.15\,\mu$m) were seen to occur in colonies ($\sim 4\,\mu$m diameter). These cells were characterized by the formation of a thin layer of aluminium at the cell boundaries due to breakdown of the planar stability of the interface during recalescence, resulting in a rejection of aluminium solute atoms in front of the moving interface, Fig. 3b. Near the gas side, coarse particles of Al_6Mn were precipitated directly from the melt followed by solidification of the remaining melt liquid into the icosahedral phase, Fig. 3c. Small islands of what is believed to be Al_4Mn [2] are also seen in this figure though the corresponding electron diffraction pattern brings out strong reflections due to Al_6Mn.

A different type of electron diffraction pattern was obtained from crystals located in zone A. The pattern, Fig. 4a, was reported by Shechtman *et al.* [2] as a precipitate in dilute Al–Mn alloys having 5 Mn and termed the T-phase, having an undetermined complex structure. As can be seen, the pattern is marked by a translational periodicity in one direction and a periodicity corresponding to a quasi-crystal in the other direction. We believe this to be a type of incommensurate phase which is closely related to the icosahedral structure. Bendersky [4] has reported that this phase has a non-crystallographic point group 10/m (or 10/m m m) together with long-range orientational order and one-dimensional translational symmetry. The growth morphology of this phase from the melt is cylindrical with the ten-fold rotation axis lying along the cylinder axis. The image of this phase is shown in Fig. 4b.

Another diffraction pattern, consistent with the 10/m point group form is given in Fig. 5a. For comparison an electron diffraction pattern of the

Figure 2 Scanning electron micrograph through the thickness of the as-melt-spun ribbon.

TABLE I Measured d values for various peaks in the X-ray diffraction pattern for as-melt-spun ribbon

Observed d (nm)	Phase*	Observed d (nm)	Phase*
0.435 6	Al_4Mn	0.2023	Al
0.386 3	I	0.1494	I
0.344 3	–	0.1459	I
0.242 2	–	0.1431	Al
0.233 9	Al	0.1306	–
0.225 3	Al_6Mn	0.1272	I
0.216 57	I	0.1220	I
0.208 01	Al_6Mn	0.1098	I
0.206	I	0.1084	I

*Phases are identified on the basis of d values reported in the literature (see [5] for icosahedral (I) phase and ASTM data for the others). Underlined values are those for which the relative intensity (I/I_0) is maximum.

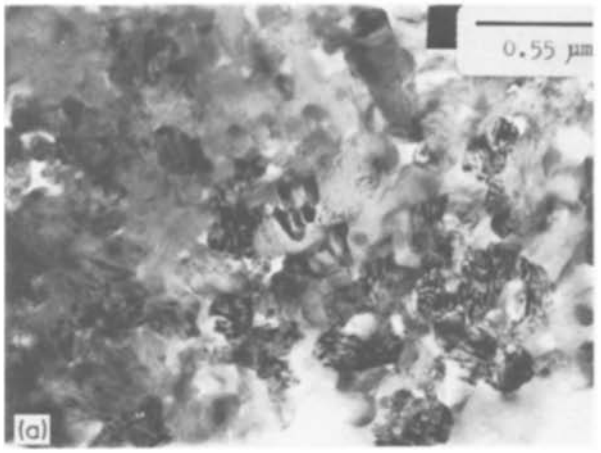

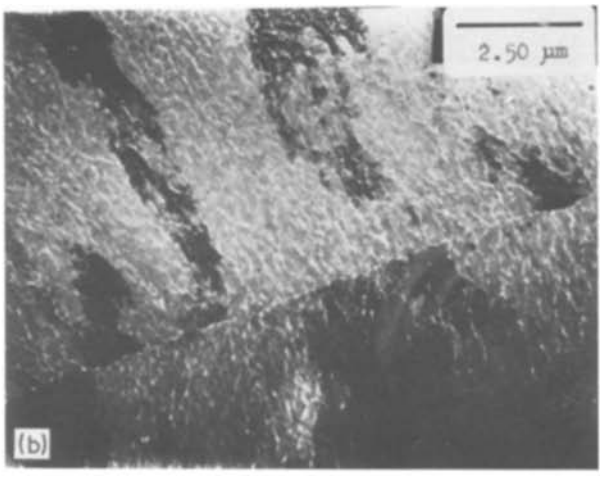

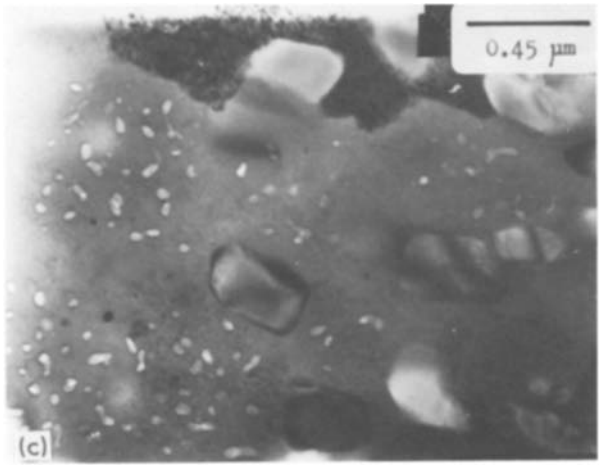

Figure 3 Transmission electron micrographs for the as-melt-spun ribbons: (a) zone A, (b) zone B near the ribbon centre, (c) zone B near the gas side.

icosahedral phase (with long-range orientational order and non-crystallographic point group symmetry $m\bar{3}\bar{5}$) in five-fold symmetry is displayed in Fig. 5b. Considering only the strongest spots, we can easily find that the angle between the radial rows in Fig. 5b is exactly 36°, whereas these angles in Fig. 5a are approximately 35° and 37° and the spots are not exactly collinear. From Fig. 5a the readings given in Table II were obtained.

From Table II, the unindexed peaks in Table I are now identifiable and one can assess the overlap that can take place between the true five-fold symmetry and the almost five-fold symmetry corresponding to the so-called T-phase or decagonal phase (hereafter referred to as the decagonal phase). For example, the reflection at 0.206 nm in the above pattern could well be related to the 0.2066 nm reflection from the icosahedral phase.

Bright- and dark-field micrographs, using the transmitted beam and a diffracted beam from spot no. 4 (0.2096 nm) are displayed in Figs 5c and d, respectively. These two micrographs reveal the presence of a high density of planar defects, thus explaining the streaking observed in Fig. 5a. Such is not the case for the icosahedral structure as will be discussed later. We believe that these defects in the decagonal phase are microtwins in the form of sheets normal or inclined to the plane of the micrograph.

Fig. 6a is a higher magnification micrograph of the icosahedral phase displayed previously in Fig. 3b. The structure is characterized by the absence of visible details and seems to be featureless. Fig. 6b is the same structure after bringing it into a two-fold symmetry position by tilting. No signs of twins or

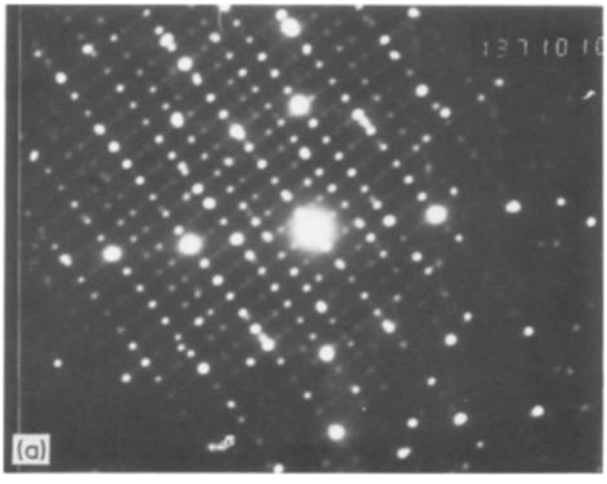

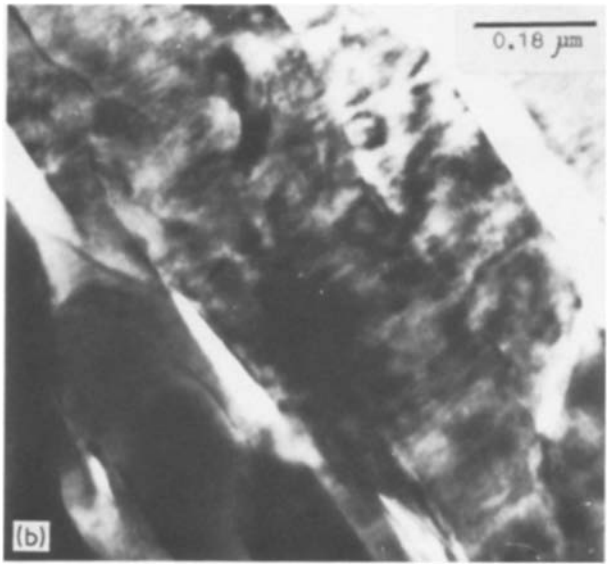

Figure 4 Transmission electron micrographs corresponding to zone A: (a) SAD, (b) BF, showing the presence of faults normal to the plate growth direction.

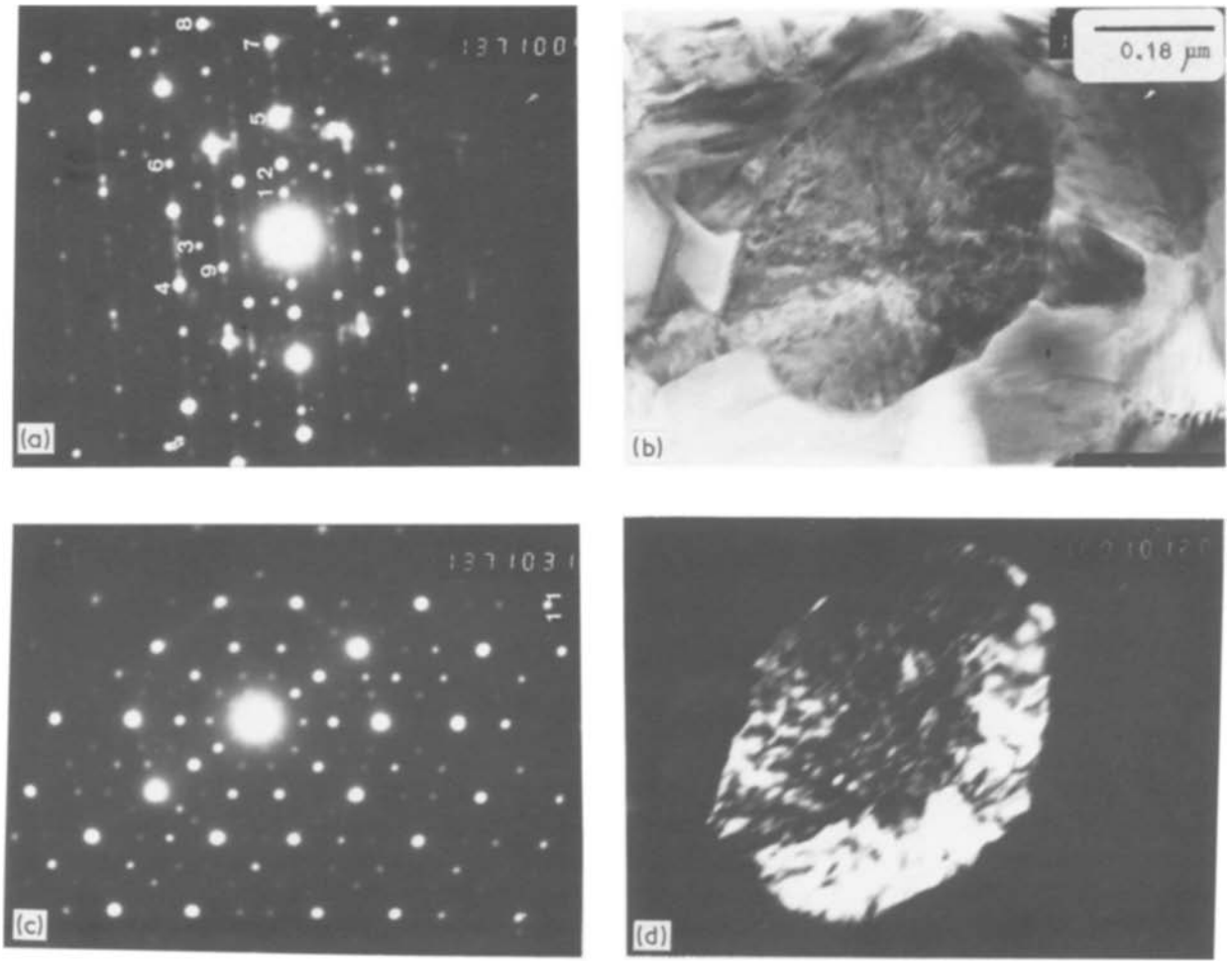

Figure 5 Transmission electron micrographs corresponding to zone A: (a) SAD showing almost five-fold symmetry; (b) SAD showing true five-fold symmetry; (c) BF and (d) DF of the decagonal phase using (a). Note the presence of intensive faults normal to the electron beam direction.

microcrystallinity are detectable from this micrograph. The electron diffraction pattern corresponding to Fig. 5a (taken from an area about 0.6 μm diameter) is shown in Fig. 7a. This diffraction has been described by Portier *et al.* [6] to be the (1 1 0) orientation with the bright spots ($\sim$0.2084 nm) slightly displayed from the average host lattice. The homothetic scaling in this case is τ^3, where τ is the well-known golden mean ($\tau = 1.618$). On tilting the crystal to a two-fold symmetry position, Fig. 7c, an intermediate SAD is viewed, Fig. 7b, characterized by long-range orientational order with no lattice translational symmetry. The intensities of alternately occurring rows of faint and bright spots may be attributed to their respective structure factors.

3.2. Effect of annealing

The following observations could be made from X-ray

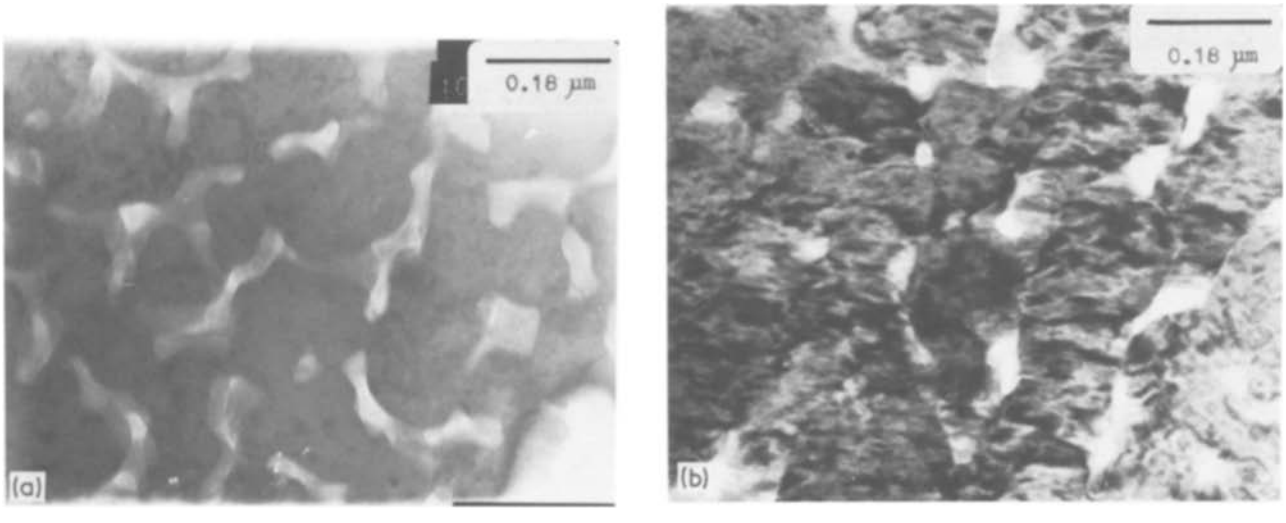

Figure 6 Transmission electron micrographs of the icosahedral phase: (a) before tilting; (b) after tilting into two-fold symmetry.

TABLE II Measured d values for various spots in the electron diffraction pattern shown in Fig. 6a

Spot no.	d (nm)	Spot no.	d (nm)
1	0.528	5	0.2067
2	0.342	6	0.188
3	0.243	7	0.1308
4	0.2096	8	0.110

diffraction patterns obtained from ribbons annealed for 1 h at 400, 450 and 500° C.

1. The complete disappearance of Al-peaks, indicating its transformation into Al_6Mn as a result of the rejection of the excess of manganese atoms. This is also reflected in the associated increase in the microhardness to 5500 MPa.

2. The persistence of the decagonal phase, as inferred from the appearance of the 0.206 nm peak (the strongest spot in Fig. 5a) as a separate line in the specimen annealed at 500° C/1 h.

3. The great reduction in the amount of icosahedral phase (see line 0.216 57 nm corresponding to maximum intensity in Table I) at the cost of the increase in the intensity of Al_6Mn. However, the icosahedral phase was still visible after 500° C/1 h.

4. The noticeable shift in the position of the line corresponding to the (3 1 0)-Al_6Mn plane from 0.208 26 nm (at the stoichiometric composition) to 0.2092 nm at 450° C or 0.209 nm at 500° C. This shift may be due to the mixing up of more than one phase, i.e. Al_6Mn, Al_4Mn and decagonal phases.

TABLE III Observed peaks in X-ray diffraction patterns for Al–27% Mn ribbons at different annealing treatments

400° C/100 h	450° C/100 h	500° C/100 h	600° C/1 h
0.493 49	0.493 1	0.493 1	0.512 54
0.432 2	0.442 9	0.442 9	0.248 09
0.376 7	0.347 7	0.348 9	0.232 2
0.346 75	0.330 8	0.329 6	0.227 22
0.330 65	0.262 2	0.262 1	0.217 99
0.262 4	0.253 8	0.254	0.215 4
0.253 58	0.242 3	0.246 2	0.212 68
0.242 33	0.226 7	0.242 9	0.211 2
0.226 2	0.221 8	0.226 6	0.206
0.215 6	0.218 6	0.221 2	0.203 4
0.208 5	0.215 7	0.218 6	0.202 2
0.202 6	0.208 5	0.215 61	0.130 41
0.189 1	0.205 9	0.208 5	0.127 46
0.183 9	0.202 7	0.205 9	0.125 92
0.147 1	0.189 2	0.203	
0.145 9	0.165	0.189 3	
0.141 5	0.149 1	0.130 8	
0.135	0.147 2	0.128 2	
0.130 8	0.141 6	0.124 06	
0.128 0	0.128 1		
0.127 1	0.126 1		
0.124 0	0.125 3		
0.122 7	0.124 0		
0.117 6	0.122 6		
0.14	0.114 3		
0.111 69	0.111 63		
0.108 4	0.108 3		
	0.107 6		

Note: Underlined values are those for which the relative intensity (I/I_0) is maximum.

Table III summarizes the basic lines after 100 h annealing at the same temperatures. The main observations that could be made from this table are: (1) the complete disappearance of the icosahedral phase; (2) the persistence of the decagonal phase (0.2059 nm) up to 100 h at 500° C; (3) the reduction in the d-value corresponding to (3 1 0)-Al_6Mn to 0.2085 nm, approaching the stoichiometric value 0.208 26 nm; (4) either the increase in the d-value of the spot no. 2 in Fig. 5a from 0.342 nm, in the as-melt spun condition to 0.348 nm at 500° C/100 h or the reduction in the d-value of spot 9 from 0.352 nm to the mentioned value. This change may be explained in terms of the change in the range

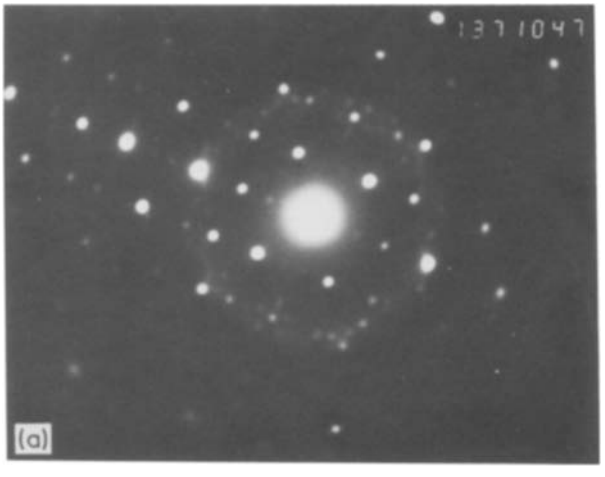

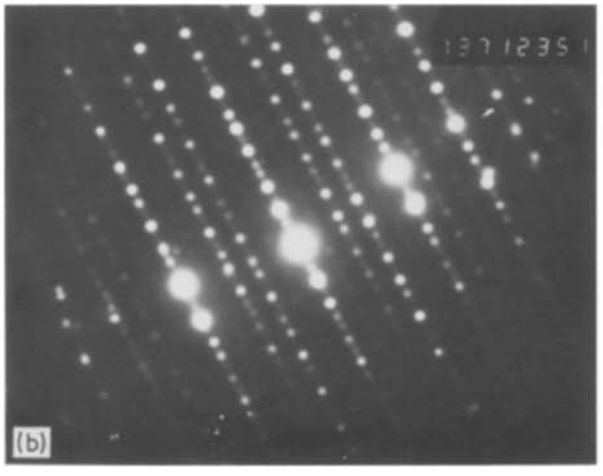

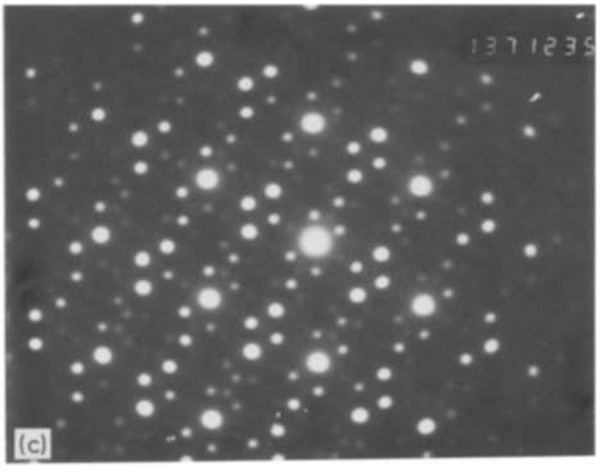

Figure 7 A series of SADs taken from: (a) Fig. 6a, (c) Fig. 6b, (b) an intermediate stage.

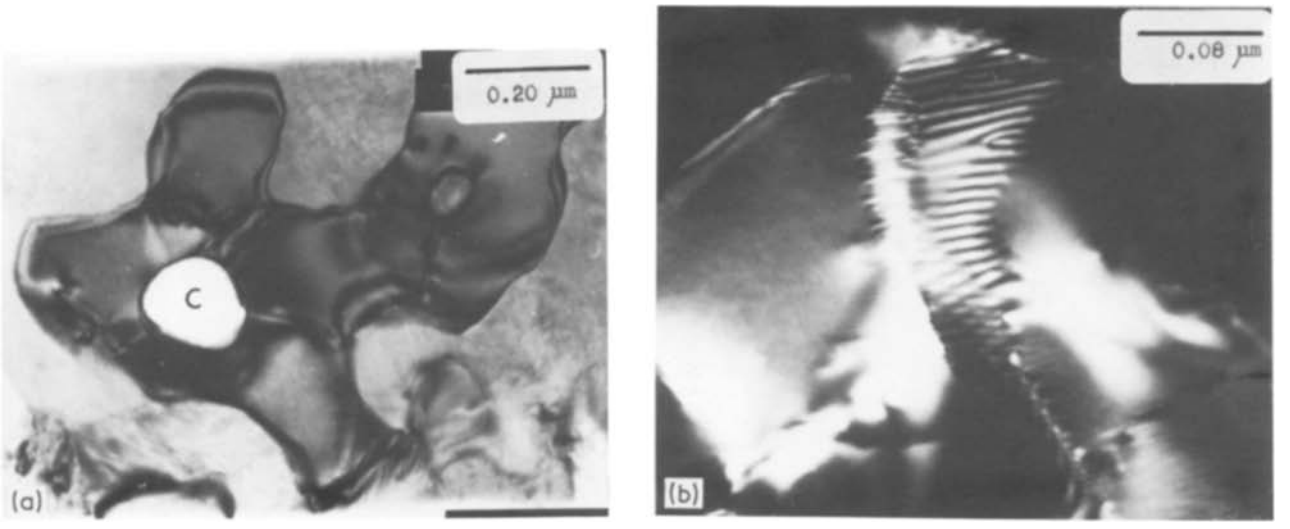

Figure 8 Transmission electron micrographs following annealing at 400° C/1 h, showing: (a) crystallization of the icosahedral phase; (b) dislocation arrangements at the grain boundary.

of the incommensuration of the phase shown in Fig. 5 or the formation of another decagonal phase.

An interesting observation made from the specimen annealed for a short time, 1 h, at 600° C is that the position of maximum intensity changes from (3 1 0)-Al_6Mn to (44.5)-Al_4Mn. This is coupled with the presence of the line at 0.206 nm of the decagonal phase. However, the fact that the crystal structure of Al_4Mn is almost completely unknown complicates the indexing.

Fig. 8a represents the microstructure of an area as that shown in Fig. 3c after subjecting to annealing 1h at 400° C. As can be seen, the matrix (icosahedral phase) has crystallized into the Al_6Mn phase, with grains about 0.2 μm diameter. Two microstructural observations could be made from the associated dark-field micrograph, imaged on an Al_6Mn reflection from the newly formed crystal. The first was that these crystals were crystallographically different from the original Al_6Mn crystal (i.e. centre of nucleation marked C in Fig. 8a). The second, that these crystals possessed low-angle misorientation. A higher magnification micrograph, Fig. 8b, reveals the dislocation arrangement at the grain boundary. However, due to overlapping between the crystals, Moiré fringes are also observed in the same micrograph.

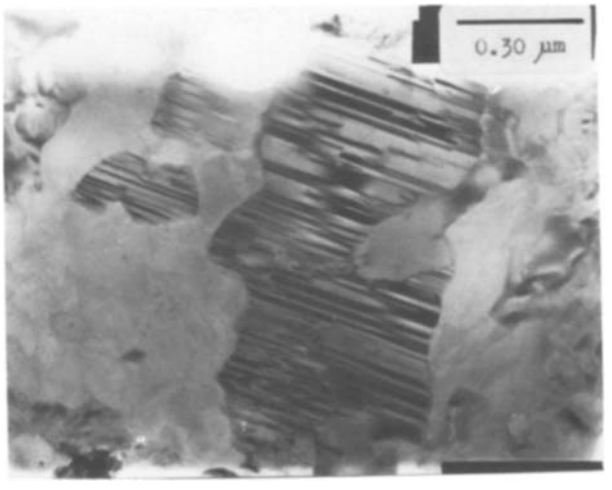

Figure 9 Transmission electron micrograph of the ribbon annealed 1 h at 450° C, obtained from the decagonal phase, revealing the presence of several domains within a plate of the decagonal phase. Note the change in the direction of the faults at the domain boundary.

In good agreement with the observation made by X-ray measurements on the persistence of the decagonal phase after annealing, Fig. 9a reveals longitudinal crystals (about 1 μm long and 0.3 μm wide) with planar defects perpendicular to the growth direction of these crystals. In this micrograph, partial crystals are also visible since they are inclined to the foil plane. These grains exhibit several domains that cause marked kinks in the direction of the defects at the domain boundary (arrowed). The corresponding SAD exhibited the essential features that were reported earlier in Fig. 4a.

In the same foil but away from the area shown in Fig. 9, the dark-field micrograph of Fig. 10a reveals a striking feature in that an almost regular shaped crystal is viewed, containing several domains with planar defects of unequal spacing and with fine fringes covering the entire grain. The widths of the bands of the fringes are much smaller in area A than those in area B. A higher magnification of area A, Fig. 10b, taken at the grain boundary, reveals the presence of microtwins which give rise to a stacking fault-like contrast and wedge-shaped fringes at the boundary. The diffraction pattern corresponding to these micrographs (Fig. 10) displays parallel equidistant rows of closely spaced spots. The direction of these rows is normal to the direction of the microtwins. It is known that the presence of planar intensity in reciprocal space can be due to the presence of one-dimensional objects in real space, aligned normal to the planes.

Coming to area B, Fig. 10c, one observes the presence of twins (dark bands) separated by large bands of fine fringes. Since the first and last fringes in these bands have the same contrast (bright–bright or dark–dark), this leads us to believe that they are δ fringes (for details see Whelan [7]). Kinks in the otherwise parallel nature of these fringes indicate the domain boundaries, as for example, shown by the arrows in the left-hand corner of Fig. 10c.

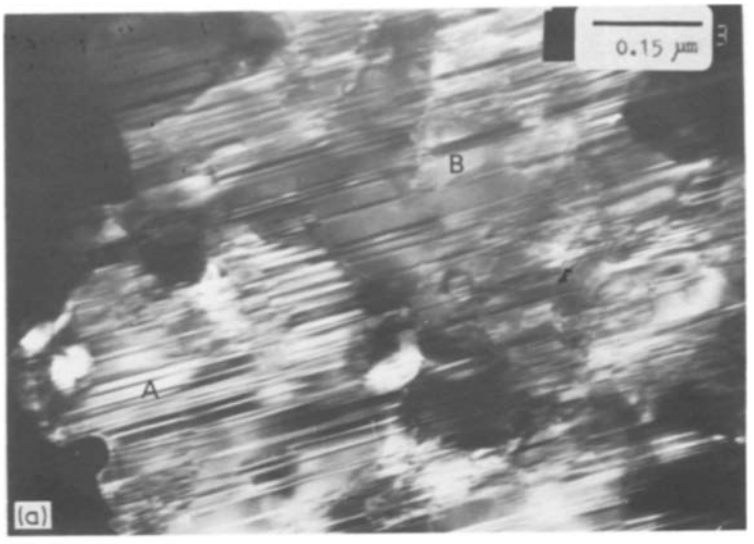

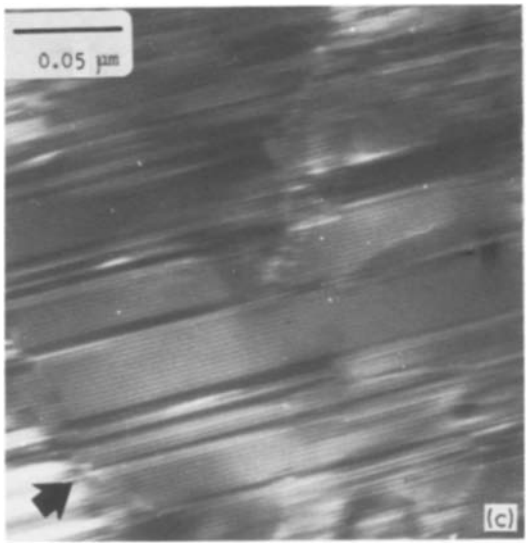

Figure 10 Dark-field micrographs for a decagonal phase particle, revealing (a) the presence of microtwins and stacking fault-like contrast, (b) high magnification micrograph corresponding to area A in (a), (c) high magnification micrograph corresponding to area B in (a).

Combining Figs 9 and 10 leads to the conclusion that the twin sheets are inclined with respect to the electron beam direction. Given the fact that a longitudinal section with inclined twins has never been reported either in earlier [8] or the present work, we believe that the crystals displayed in Fig. 9 are *plates* and not *cylinders*. Also, Fig. 10 is not the cross-section of Fig. 9. This means that we are dealing with two or more sets of decagonal phases having different morphologies. On the basis of the foregoing discussion we cannot rule out the possibility that the decagonal phase may form by multiple twinning of conventional crystals. The extensive presence of the planar faults may, however, destroy the appearance of the microtwins.

For the treatment at 450° C/1 h, a large number of the electron diffraction patterns obtained could be indexed on the basis of Al_4Mn. Another morphology of the decagonal phase is displayed in Fig. 11, where the phase is seen to form by growth on the surface of the icosahedral cells.

Fig. 12 shows the microstructure following annealing at 500° C for 100 h. As can be seen, several areas are intensely faulted and exist along with Al_6Mn and Al_4Mn islands (upper left side). Diffraction patterns taken from areas A and B exhibited almost five-fold symmetry. It was always observed that in one particular direction, the distance between two spots (on the circle) was larger than along other directions. For example in Fig. 5a, the value varies between 0.2096 and 0.2067 nm, while for Fig. 12 it varied between 0.214 and 0.209 nm.

It is interesting to note in this connection that

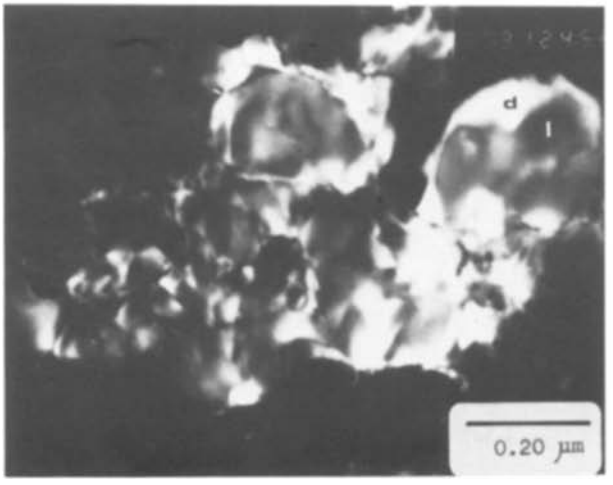

Figure 11 Dark-field micrograph showing the growth of the decagonal phase on the surface of the icosahedral phase.

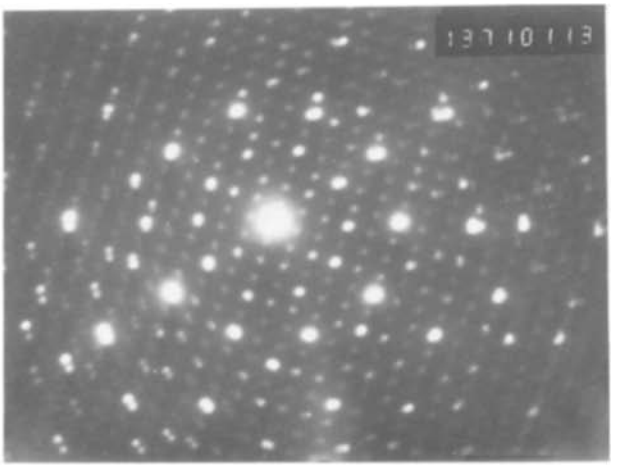

Figure 13 SAD obtained from the ribbon annealed 1 h at 600° C showing Al_4Mn phase along with the decagonal phase oriented near five-fold symmetry. Note the coincidence between the spots of the two phases.

Knowles *et al.* [9] have reported that they obtain a larger interplanar spacing of $d = 0.214$ nm for the true five-fold symmetry pattern (obtained by high-resolution electron microscopy) of the icosahedral phase in $Al_{86}Mn_{14}$ (atomic composition), compared to 0.2062 nm reported by Shechtman and Blech [3]. In our case, however, such a variation is less pronounced.

Figure 13 is a diffraction pattern of Al_4Mn at the $[0\,1\,\bar{1}\,1]$ zone axis and produced from a specimen annealed 1 h at 600° C (the temperature at which Al_4Mn is dominating the microstructure, see Table III). Reflections due to the decagonal phase in five-fold symmetry are clearly visible in the same diffraction pattern. The presence of planar defects gives rise to some sort of splitting of the Al_4Mn spots. It is thus suggested that, due to atomic displacement, transformation from a commensurate into an incommensurate structure can take place.

Based on our own observations as described above, a comparison can be made between the icosahedral and decagonal phases as shown in Table IV.

4. Conclusions

From the results obtained in the present investigations and keeping in mind our earlier work [10] on Al–14 wt % Mn ribbons where the icosahedral phase was found to occur (and where Al_6Mn was the resulting equilibrium phase), we draw the following conclusions:

1. Increasing the manganese content from 14% to 27% results in the formation of another quasistructure, i.e. the decagonal phase, in addition to the icosahedral one. This structure exhibits an almost five-fold symmetry similar to the true five-fold symmetry of the icosahedral structure, and belongs to the 10/m (or possibly 10/m m m) point group (cf. $m\,\bar{3}\,\bar{5}$ for icosahedral phase).

2. While the icosahedral phase reveals no morphological difference and occurs directly from the melt, the decagonal phase is seen to exhibit different morphologies and can occur from the melt or grow on the surfaces of the icosahedral phase. Of these, one of them is plate-like, with the plates inclined to each

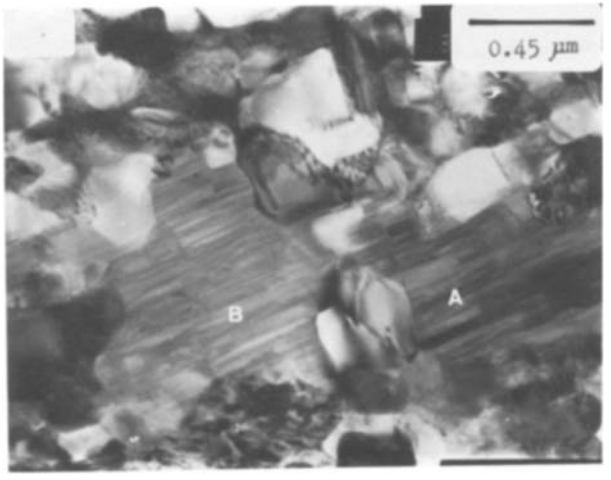

Figure 12 Transmission electron micrograph obtained from the ribbon annealed at 500° C–BF.

TABLE IV Comparison between the icosahedral and decagonal phases

	Icosahedral phase	Decagonal phase
1.	$m\,\bar{3}\,\bar{5}$ point group symmetry	10/m or possibly 10/m m m point group symmetry
2.	Exhibits true five-fold symmetry with diffraction spots spaced at equal intervals of 36° between radial rows	Exhibits almost five-fold symmetry; Angle between radial rows varies between 35° and 37°; Also, spots are not exactly collinear
3.	All spots lie exactly on the same circle for a particular ring of given d value	A slight deviation ($\pm 2\%$) is always observed
4.	Faults or twinning never observed within the grains	Heavily faulted with several domains within the grains and with occasional appearance of microtwins
5.	Occurs directly from the melt	Can occur from the melt or at the surfaces of the icosahedral grains
6.	Crystallizes into Al_6Mn starting from 400° C	Still stable up to 500° C/100 h; Exists along with Al_4Mn at 600° C

other. Within the grains of the decagonal phase, several domains are observed containing a high density of planar faults. Since microtwins are also observed within the grains, the possibility that the decagonal phase may form by multiple twinning cannot be completely neglected.

3. The effect of annealing (400 to 600° C/1 to 100 h) shows that the icosahedral phase becomes unstable at 400° C/1 h, crystallizing into Al_6Mn. The decagonal phase is seen to persist, even after 500° C/100 h. The existence of the decagonal phase at 600° C together with the Al_4Mn phase suggests that the decagonal phase arises from a commensurate → incommensurate transformation due to atomic displacement within the Al_4Mn phase. In other words, the presence of the icosahedral and decagonal phases is related to the equilibrium structures present at a particular concentration of manganese in the given Al–Mn alloy. Thus, at 14% Mn only the icosahedral phase is observed (Al_6Mn being the only equilibrium structure), while at 27% Mn, both icosahedral and decagonal phases are found to occur (Al_6Mn + Al_4Mn occurring in equilibrium).

References

1. D. SCHECHTMAN, I. BLECH, D. GRATIAS and J. W. CAHN, *Phys. Rev. Lett.* **53** (1984) 1951.
2. D. SHECHTMAN, R. J. SCHAEFER and F. S. BIANCANIELLO, *Met. Trans. A* **15A** (1984) 1987.
3. D. SCHECHTMAN and I. A. BLECH, *ibid.* **16A** (1985) 1005.
4. L. BENDERSKY, *Phys. Rev. Lett.* **55** (1985) 1461.
5. P. A. BANCEL, P. A. HEINEY, P. W. STEPHENS, A. I. GOLDMAN and P. M. HORN, *ibid.* **54** (1985) 2422.
6. R. PORTIER, D. SHECHTMAN, D. GRATIAS and J. W. CAHN, *J. Microsc. Spectrosc. Electron.* **10** (1985) 107.
7. M. J. WHELAN, "Diffraction and Imaging Techniques in Materials Science", Vol. 1, edited by S. Amelinckx, R. Gevers and J. Van Landuyt (North-Holland, Amsterdam, 1978) pp. 43–106.
8. J. A. KNAPP and D. M. FOLLSTAEDT, *Phys. Rev. Lett.* **55** (1985) 1591.
9. K. M. KNOWLES, A. L. GREER, W. D. SAXTON and W. M. STOBBS, *Phil. Mag. B* **52** (1985) L31.
10. F. H. SAMUEL, A. M. SAMUEL, A. DE JONCKERE and F. GERIN, *Met. Trans. A* (1986) in press.

Received 30 December 1985
and accepted 30 June 1986